

Light-scattering test of parametric equations of state near the critical point of carbon dioxide

Pilwon Kang* and John A. White†

Department of Physics, The American University, Washington, D.C. 20016

(Received 2 April 1984)

Light-scattering measurements are reported for densities and temperatures close to the critical point of CO₂ in the range $|(T-T_c)/T_c| \leq 10^{-4}$. A contour of constant scattering was determined in the z - T plane, where z is the vertical distance from the point of maximum scattering or from the meniscus at the given temperature. The contour was found to be fitted by a cubic model parametric equation with $a=22.3$, $\gamma=1.22$, $\beta=0.347$, $b^2=3/(3-2\beta)=1.30$, $T_c=31.01155^\circ\text{C}$, and $r=6.45 \times 10^{-5}$. The measured contour was also compared with predictions of a parametric equation of state representing interferometric measurements made very close to the critical point and with linear model equations that have been used to describe thermodynamic measurements made farther from the critical point. Disagreements amounted to as much as 4%, a portion of which may be attributed to the difficulty of completely eliminating vertical temperature gradients in the scattering cell. Data are also presented for several profiles of scattering intensity versus height and for maximum scattered intensity versus temperature near the critical point.

I. INTRODUCTION

In a previous investigation,^{1,2} light scattering was studied as a function of density as well as temperature to determine an empirical, scaling-law equation of state for carbon dioxide close to its critical point. Good qualitative agreement was found with a parametric model equation of the type proposed by Josephson³ and Schofield,⁴ using values for the parameters of the model extrapolated from light-scattering and thermodynamic data obtained farther from the critical point.²

The present investigation was undertaken to determine the equation of state to improved accuracy and to test alternative linear^{4,5} and cubic⁶ parametric models. The work reported here complements the interferometric investigation of Hocken and Moldover,⁷ which was performed over a similar range of density and temperature. Some discrepancies between the results of the two experiments are noted. They amount at most to a few percent but lie outside the combined estimated errors for the two experiments. Brief reports of portions of the present research have appeared previously,^{8,9} some details can be found in the dissertation of one of the authors.¹⁰

II. EQUATION OF STATE; CONTOUR OF CONSTANT SCATTERED INTENSITY

The parametric model equations for the temperature, mass density, and height coordinates of a single component fluid close to its critical point are^{4,5}

$$\begin{aligned}\Delta T &= T_c r (1 - b^2 \theta^2), \\ \Delta \rho &= k \rho_c r^\beta f(\theta), \\ \Delta z &= (a P_c / g \rho_c) r^{\gamma + \beta} (\theta - \theta^3).\end{aligned}\quad (1)$$

Here ΔT and $\Delta \rho$ are temperature and density distances from the critical point and Δz is the height relative to that

at critical density or the meniscus; r and θ are the parametric variables; a , β , γ , and k are dimensionless constants; T_c , ρ_c , and P_c are the temperature, density, and pressure at the critical point; g is the acceleration of gravity. Two simple forms of the function $f(\theta)$ have been proposed. In the linear model⁵ (hereafter abbreviated LM), one has $f(\theta)=\theta$, the consequence of which is that C_v (specific heat) $\propto r^{-\alpha}$; thus C_v does not depend on θ . In the cubic model (CM),⁶ $f(\theta)=\theta + c\theta^3$ and χ (susceptibility) $\propto r^{-\gamma}$.

At nonzero scattering angles, according to the theory of Ornstein and Zernike¹¹ (OZ), the scattered power is given by

$$P_s = C P_0 k_B T \chi \left[\frac{\partial \epsilon}{\partial \rho} \right]_T^2 (1 + q^2 \xi^2)^{-1}, \quad (2)$$

where C is a constant partially dependent upon the apparatus, P_0 the incident power, k_B the Boltzmann constant, ϵ the dielectric constant, q the scattering wave vector, and ξ the correlation length. Here, $q = (4\pi n / \lambda) \sin(\phi/2)$, where n is the refractive index, λ the wavelength, and ϕ the scattering angle. The intensity ($I \propto P_s / P_0$) of light scattered through a sufficiently small angle under conditions of constant $\partial \epsilon / \partial \rho$ is proportional to χ . Thus, a contour of constant small-angle scattered intensity as a function of (z, ρ, T) close to the critical point can be expected to be a contour of constant χ to the extent that the remaining factors in the OZ formula do not vary appreciably along the contour. For the cubic model, this contour is given by Eq. (1) with r set equal to a constant. In general, the contour of constant χ is a path of "isocline," with $\partial \rho / \partial z = \text{const}$. In the work reported here, such a thermodynamic path (path of isocline) was obtained in the (z, T) plane from measurements of individual isothermal I versus z profiles at a fixed scattering angle of $\phi = 14.0^\circ$ as measured externally to the scattering cell. The particular isocline was chosen such that it crosses the

temperature axis at $T_{\min} \approx T_c - 0.006^\circ\text{C}$ and $T_{\max} \approx T_c + 0.020^\circ\text{C}$.

If true scaling-law behavior has been reached already at $|t| \lesssim 7 \times 10^{-5}$ then an isocline measured there should largely determine the equation of state and singular part of the free energy density; an isocline closer to the critical point would be of the same shape, but with the aspect scaled by the exponent $\beta + \gamma$.² A separate determination of the slope $(\partial\rho/\partial z)_T$, i.e., the magnitude of the isocline, would complete the specification of the equation of state and singular part of the free energy density.² The slope could be found by applying corrections for multiple scattering and attenuation,¹² or by measuring the vertical deflection of the transmitted light. The analysis of data obtained in the present investigation has been limited to finding the locus of the isocline.

The path of the isocline investigated here can be expected to differ from a contour of constant scattered intensity by at most a few percent. For this isocline, the correlation length^{13,14} $\xi \sim 1.5A(\Delta T/T_c)^{-0.63}$ yields $q^2\xi^2 \sim 0.03$ on the critical isochore, and thus results in a 3% reduction of scattering via the factor $1 + q^2\xi^2$ in the denominator of the OZ expression. The correlation length is not expected to be constant along an isocline path,¹⁵⁻¹⁷ its variation may result in a change of the factor $1 + q^2\xi^2$ by 1% along the isocline. Corrections¹⁵ to the q^2 dependence in the OZ expression are of the order $q^4\xi^4$ and are negligible when $q^2\xi^2 \sim 0.03$. The change in q^2 at fixed scattering angle due to the variation in the refractive index is less than 1% and hence contributes negligibly to $q^2\xi^2$. The geometrical effects due to the bending of the scattered light in a horizontal plane as it passes from the fluid into the air on the way to the detector, combined with the contribution from the factor¹⁸ $(\partial\epsilon/\partial\rho)_T^2 = (n^2 - 1)^2(n^2 + 2)^2/9\rho^2$ differ by $\sim 1\%$ between gas and liquid portions of the isocline; however, they cancel when the two branches of the isocline are averaged, yielding a net error from these sources of substantially less than 1%.¹⁰ A complete analysis of light scattering done at a reduced temperature of $|t| = |(T - T_c)/T_c| \lesssim 7 \times 10^{-5}$, as in the present experiment, requires consideration of multiple scattering and attenuation of the light in the scattering cell. These effects are not negligible,^{12,19} but along an intensity contour they remain approximately constant, the chief source of nonconstancy being the variation of attenuation due to the anticipated variation¹⁵ of ξ along a contour. In the present experiment, neither the attenuation nor ξ was measured and consequently no correction has been applied for the variation of the attenuation which would result from a nonconstant ξ along the contour. In future work, it is planned to modify the experimental apparatus to be able to measure the attenuation and also ξ . This may result in corrections of contour data amounting to $\geq 1\%$. In view of the estimates given above, it is anticipated that apart from the ξ -dependent attenuation correction the intensity contour should reproduce the thermodynamic isocline to an accuracy of $\lesssim 1\%$.

III. EXPERIMENTAL ARRANGEMENT

The experimental arrangement was basically the same as that used for earlier work.^{2,19} The scattering cell was

cylindrical, with its symmetry axis parallel to the laser beam. It was made of a stainless-steel bellows, ended by coated sapphire plates. The laser light was polarized perpendicular to the scattering plane and the étalons of the cell were optically oriented to prevent depolarization of light scattered in the horizontal plane. The volume of the cell could be varied by means of an oil press which, by virtue of the elastic bellows, was capable of adjusting the window separation which is 5 mm under no stress. The cell and oil press assembly was enclosed in a double thermostat. The inner stage was an aluminum cylinder, which was placed concentric with the cell and acted as a thermal shield as well as a heater with nichrome wires on it. The cell-oil-press assembly was attached to the shield by three nylon screws, with a 1-cm air gap between the shield and cell assembly. The outer stage was a light-tight, water-heated box which housed the entire light-scattering arrangement except for the laser light source.

The optical arrangement is shown in Fig. 1. A silicon photocell mounted inside the temperature-controlled box was used to monitor the incident light from a 0.5-mW He-Ne laser to better than 0.5% accuracy at all times. Scattered intensities (I) were recorded as ratios of the output current from the RCA 7265 photomultiplier, used to detect the scattered light, to the output current from the Si cell.

The photomultiplier tube was calibrated by placing in and out of the laser beam a neutral density filter whose attenuation factor had been previously calibrated, and by noting the ratio of the photomultiplier tube (PMT) output currents with and without the filter. This measurement was done for a variety of incident light intensities. At the input voltage of 1500 V used for the entire contour experiment, the PMT calibration was linear to 1% between $I=2$ and 160 on a chosen arbitrary scale. Although no corrections were needed for the contour measurements done at $I=60$, large intensity values up to $I=380$ obtained near the critical height at temperatures very close to T_c had to be corrected upwards by as much as 15%, with an error bar of up to 2%.

The sensitivity of the PMT was checked at the end of each day's experiment by switching the light beam from path 1 to path 2 (see Fig. 1). The checking was done during the data-taking period of three months, throughout which time the input voltage to the PMT was maintained

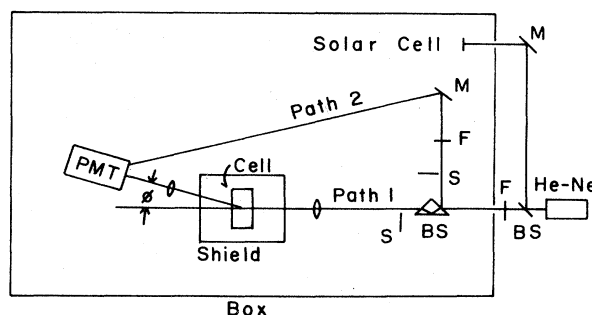


FIG. 1. Optical arrangement. BS, beam splitter; F, filter; M, mirror; S, shutter. Silicon solar cell was used to monitor the laser power. Light path 2 was used to check PMT sensitivity.

at 1500 V. The sensitivity was found to remain constant within $\pm 1\%$.

The temperature of the scattering cell was measured with a Natl. Bur. Stand. (U.S.)—calibrated Leeds and Northrup platinum thermometer attached to the oil press. The estimated accuracy was ± 2 m°C for absolute temperature and ± 0.1 m°C for reproducibility. The thermister-operated temperature control of the inner thermostat was stable to ± 0.1 m°C over several days as measured by this platinum thermometer.

As measured from the time when the thermometer came to within ± 0.1 m°C of an equilibrium temperature, the half-time for the height profile to relax to a final state was not more than several hours¹⁰ for any temperature change that was brought about within the contour range. Note that the formula²⁰ $\tau = d^2/\pi^2 D$ yields ~ 7 h with the thermal diffusion distance (or the window separation) d of 0.5 cm and the diffusivity¹³ $D \sim 10^{-6}$ cm²/s.

The possible temperature gradient in the cell was estimated as follows. First we checked if there would be a change in the height (I versus z) profile as a result of a change in the difference between the shield temperature and the ambient temperature of the box. The width ($z_+ - z_-$) of a height profile is related to the gradient dT/dz :²

$$z_+ - z_- \propto \left[1 + \frac{1}{\rho g} \left[\frac{\partial \rho}{\partial T} \right]_p \frac{dT}{dz} \right]^{-1} \quad (3)$$

During repeated tests over several weeks with the box ambient set alternately at 15 m°C (where most of the contour data were obtained) and 120 m°C below the cell temperature, the variation in the width could not be observed; this indicated that there was no detectable temperature gradient due to heating of the inner thermostat.

Second, the contribution to the temperature gradient in the cell resulting from the nonuniformity of the box temperature during the period of the experiment was estimated to be $\lesssim 2 \mu\text{C}/\text{cm}$.²¹ This estimate was made by (1) artificially magnifying the box gradient and observing the variation in the height profile (this indicated that the combined shielding factor of the shield, oil press, and cell was better than 500) and (2) applying this factor to the box gradient of 1 m°C/cm which was measured at the end of the contour experiment at the shield position with the shield and its contents removed.

IV. RESULTS AND ANALYSIS OF THE CONTOUR EXPERIMENT

The results of height scans performed at 18 equilibrium temperatures to determine a contour of constant scattered intensity are given in Table I. The table shows the vertical positions z_+ and z_- for which the scattered intensity is $I = 60$. Below T_c , z_- refers to the liquid and z_+ to the vapor; above T_c , z_- and z_+ refer, respectively, to below and above the point of maximum scattering. Also indicated in the table are the values $I^{-1} dI/dz$ at z_+ and z_- . Four typical height profiles (A, B, C, D in Table I) are shown in Fig. 2.

As Table I shows, the temperature was changed between height scans sometimes downwards and sometimes upwards. The results were analyzed to detect possible hysteresis effects; however, none were detected. Also, we found no measurable effect due to equilibration times of two or more days as compared to the usual one-day settlement time.

For measurements of scattered light at a given height, the cell was translated side to side horizontally in order to average over the effects caused by dust on, and imperfec-

TABLE I. Height scan data for the contour. Number in parentheses is the probable error in the last digit or digits. Typical height profiles (A, B, C, and D) are shown in Fig. 2.

Day	Temperature (m°C above 31.0000°C)	Height at I_1 (10^{-2} mm, arb. origin)		$\frac{1}{I_1} \left \frac{dI}{dz} \right _1$ (10^{-3} mm ⁻¹)	
		z_-	z_+	at z_-	at z_+
8	29.2	206(9)	688(6)	57(2)	65(2)
9	22.8	73(6)	824(6)	152(5)	165(2)
10	6.3	430(3)	492(3)	398(32)	441(31)
11	10.9	271(3)	640(3)	317(6)	350(30)
12	16.9	136(3)	773(3)	230(6)	249(4)
13	26.9	125(6)	764(9)	98(3)	107(3)
15(C)	22.1	71(3)	818(3)	155(9)	159(8)
16	6.3	422(2)	484(2)	374(40)	414(20)
17	22.6	73(6)	813(3)	150(4)	158(4)
18	22.7	66(6)	812(6)	153(7)	154(4)
19	11.6	248(3)	638(3)	290(20)	327(6)
20	12.5	224(5)	663(3)	290(10)	309(5)
22(D)	30.0	237(9)	607(9)	44(5)	47(5)
36	22.0	166(6)	920(6)	160(2)	161(2)
37	7.6	458(3)	593(3)	360(10)	390(10)
38	30.42	377(9)	731(9)	46(6)	49(2)
40(B)	12.65	313(3)	753(3)	290(20)	280(20)
48(A)	7.77	440(2)	582(2)	357(24)	390(20)

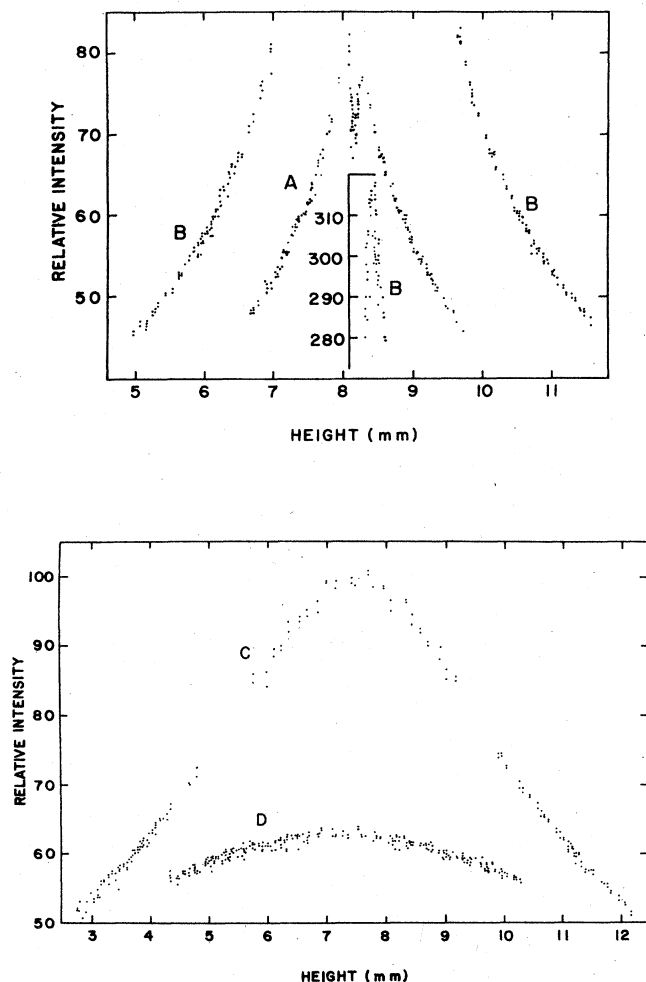


FIG. 2. Typical intensity vs height profiles used to obtain the contour. Temperatures in $^{\circ}\text{C}$ are as follows: A, 31.0078 ($\Delta T = -0.0037$); B, 31.0127 ($\Delta T = 0.0012$); C, 31.0221 ($\Delta T = 0.0106$); D, 31.0300 ($\Delta T = 0.0185$). The top of profile B is shown in the insert.

$$\chi^{-1} = \frac{aP_c}{k\rho_c^2} \frac{r^\gamma \{1 + [-3 + b^2(-1 + 2\gamma + 2\beta)]\theta^2 + b^2(3 - 2\gamma - 2\beta)\theta^4\}}{1 - b^2(1 - 2\beta)\theta^2}, \quad (4)$$

where χ^{-1} was fixed so that the χ contour would coincide with the CM r contour (line 8) at $\theta = 0, \pm 1$, i.e., at T_{\max} and T_{\min} . By so choosing the χ contours, it was possible to compare the vertical widths (z_{\max}) and the critical temperatures obtained on the basis of various model equations. The results for several sets of LM parameters are shown in Fig. 3.

Also shown in Fig. 3 is a contour of constant χ based on a parametric formulation of Wilcox and Estler²⁵ (WE) fitted to the results of the interferometric experiment of Hocken and Moldover⁷ (HM). That experiment was con-

ducted close to the critical temperature in the range $-1.5 \times 10^{-5} < t < 5 \times 10^{-5}$ comparable to the range of temperatures investigated in the present experiment ($-1.9 \times 10^{-5} < t < 6.5 \times 10^{-5}$).

ditions in, the coating of the cell windows, despite the cleaning and antidust procedures that were undertaken. Part of the scatter in the data (Fig. 2) is due to this cause. Also, data at a given height were sometimes taken at widely separated times during a run to check for the reproducibility; the result was found to be no worse than the scatter due to changing horizontal position.

Due to a slow leakage of gas ($\sim 10^{-4}$ g per week), the cell volume had to be adjusted to raise the meniscus level a few times a year; during the present work this occurred on day 29. The positions of meniscus and the maximum scattering above T_c varied in a manner consistent with this leakage and the dependence on temperature expected when the cell is filled almost but not exactly to critical density.¹⁰

The experimental contour based on the data in Table I is represented by the vertical bars in Fig. 3. The position of each bar is $(z_+ - z_-)/2$ (i.e., it is half the distance between points of equal scattering above and below the location z_c of maximum scattering). The length of each bar in Fig. 3 corresponds to the uncertainty in height measurements. The temperature measurement error for individual data points is too small to be represented in the figure. However, it appears from the data that there was a possible drift or shift of the critical temperature of the sample by $\sim 2 \times 10^{-10}$ $^{\circ}\text{C}/\text{sec}$, which amounts to 0.4 m $^{\circ}\text{C}$ over the six week duration of the contour experiment.

The data points in Fig. 3 have been fitted to a restricted CM parametric equation. With the choice² $\gamma = 1.22$, $\beta = 0.347$, and $b^2 = 3/(3 - 2\beta) = 1.30$ for three of the CM parameters, a best fit⁸ ($r = \text{const}$) was found for $a = 22.3$, $T_c = 31.01155^{\circ}\text{C}$ and $r = 6.45 \times 10^{-5}$. The result is shown in Fig. 3 as contour 8. This contour touches the temperature axis at $T_{\min} = 31.00589^{\circ}\text{C}$ and $T_{\max} = 31.03117^{\circ}\text{C}$.

In order to compare our data with the predictions of the LM, we calculated contours of constant susceptibility⁹ using LM parameters^{2,22-24} derived from thermodynamic data. To obtain a LM χ contour, Δz and ΔT values were generated as functions of r and θ by use of Eq. (1). Here r values were obtained from²

Table II summarizes some numerical data corresponding to Fig. 3. In the computer program for the LM cases, the set of parameters a , γ , β , and b^2 based on the sources listed were used to calculate z as a function of T and to determine T_c for the specified T_{\max} and T_{\min} . For the WE model, the parameters²⁶ $\theta_0 = 0.0831$, $Y_0^\beta = 0.3197$, $\Delta = 4.61$, and $\gamma = 1.24$ were used to generate a contour,

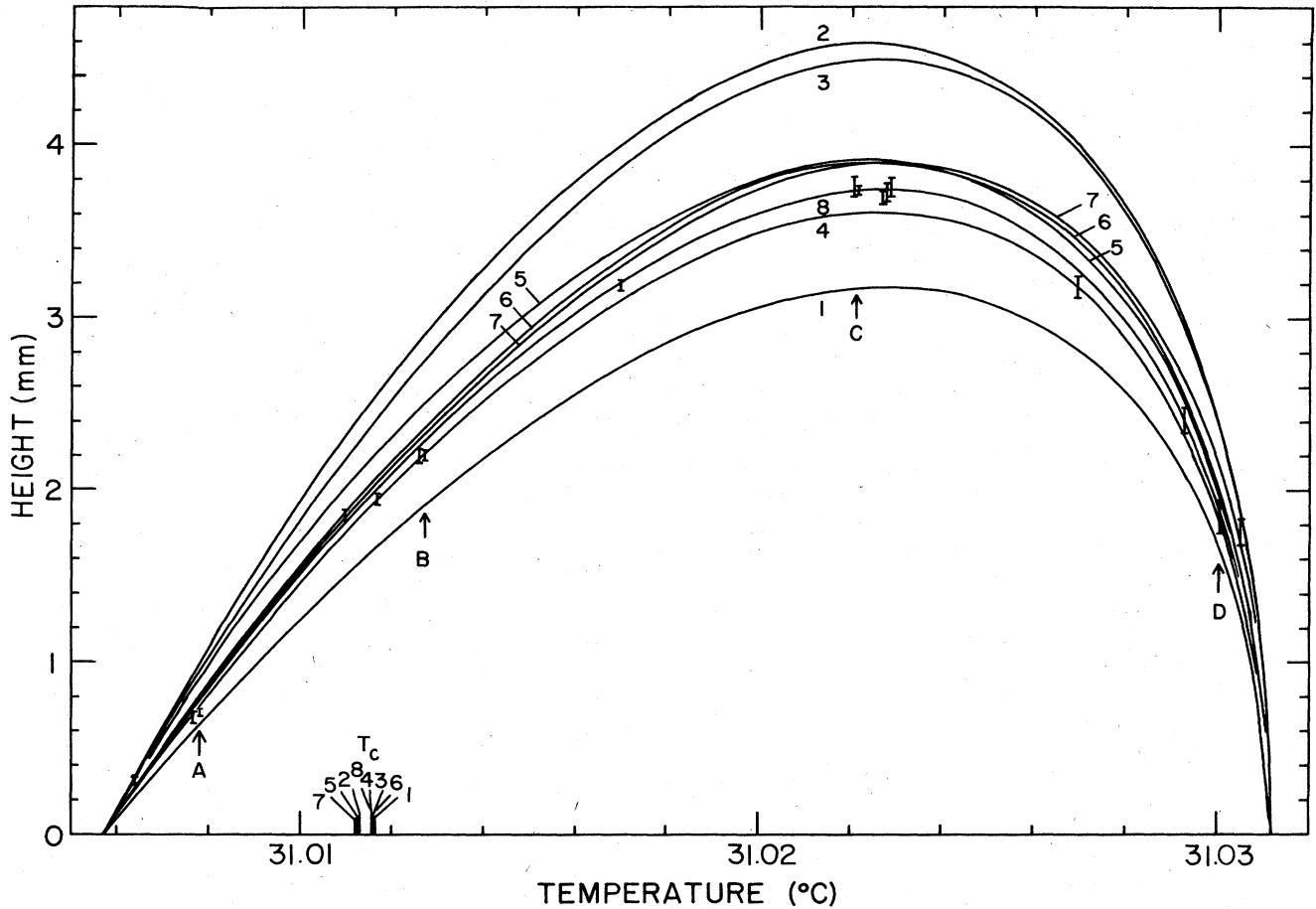


FIG. 3. Experimental contour of constant scattered intensity (vertical bars), compared with the contours computed from the model equations. 1, Hohenberg and Barmatz (Ref. 22), 1972 (restricted LM). 2, Murphy, Sengers, and Sengers (Ref. 23), 1973 (unrestricted LM). 3, MSS (Ref. 23), 1973 (restricted LM). 4, White and Maccabee (Ref. 2), 1975 (unrestricted LM). 5, Sengers, Greer, and Sengers (Ref. 24), 1976 (unrestricted LM). 6, SGS (Ref. 24) (restricted LM). 7, Hocken and Moldover (Ref. 7) (Wilcox-Estler model, Ref. 25). 8, Kang and White (Ref. 8), 1976 (CM). Contour 8 is computed for $a=22.3$, $\gamma=1.22$, $\beta=0.347$, $b^2=1.30$, $T_c=31.01155^\circ\text{C}$, and $r=6.45 \times 10^{-5}$. Data points obtained from the height scans presented in Fig. 2 are labeled A, B, C, and D.

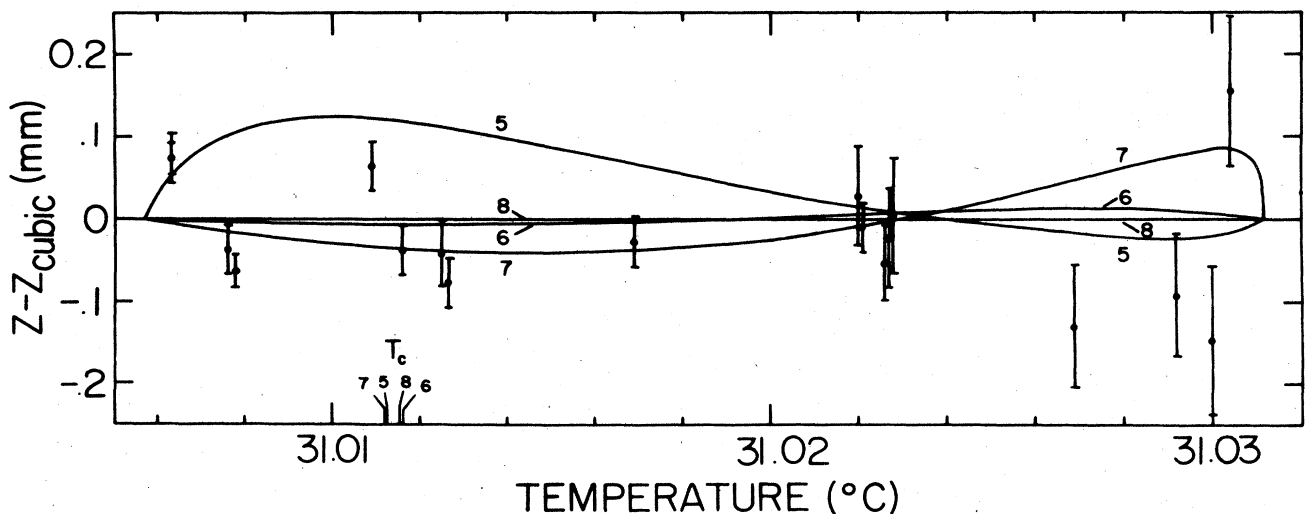


FIG. 4. Deviations in height relative to the CM contour after scaling by 4%—see text. Labels 5–8 are the same as used in Fig. 3.

TABLE II. Critical temperature and maximum value of z obtained from contour calculations. The theoretical contours were matched to the experimental contour at the temperature axis. Numbers in parentheses correspond to labels in Fig. 3. R and U refer to *restricted* and *unrestricted* models, respectively. Parameters a, γ, β, b^2 were used as input data to generate contours, except for (7), WE model (see text).

	a	γ	β	b^2	T_c (°C)	z_{\max} (mm)
(1) Hohenberg and Barmatz (Ref. 22), R-LM	28.4	1.241	0.347	1.44	31.011 63	3.18
(2) Murphy, Sengers, and Sengers (Ref. 23), U-LM	24.5	1.175	0.3486	1.70	31.011 31	4.592
(3) Murphy, Sengers, and Sengers (Ref. 23), R-LM	19.6	1.178	0.3486	1.35	31.011 60	4.51
(4) White and Maccabee (Ref. 2), U-LM	22	1.217	0.347	1.30	31.011 56	3.612
(5) Sengers, Greer, and Sengers (Ref. 24), U-LM	28.02	1.199	0.3486	1.80	31.011 25	3.917
(6) Sengers, Greer, and Sengers (Ref. 24), R-LM	21.84	1.199	0.3486	1.382	31.011 61	3.913
(7) Hocken and Moldover (Ref. 7), WE		1.24	0.321	1.277	31.011 20	3.907
(8) Kang and White (Ref. 8), CM	22.3	1.22	0.347	1.30	31.011 55	3.757

which, in the same manner as with the LM, was adjusted to match the experimental contour at the temperature axis thereby determining a critical temperature. Apart from Y_0^β these parameters may also be converted to our four-parameter set.^{27,28}

The maximum overall disagreement in T_c for the different models employed is 0.4 m°C. Although the deviations in z_{\max} from the experimental contour are quite large for some of the models, especially models 1, 2, and 3 in Fig. 3 and Table II, we wish to note that once the parameter a is adjusted to bring the computed z_{\max} to the cubic model value of 3.76 mm, all of the theoretical contours (lines 1–7 in Fig. 3) coincide with the entire CM contour, indicating a close similarity in the shapes of the contours apart from the vertical scaling factor a .

Contours based on the recent works of Sengers, Greer, and Sengers (SGS) and HM (lines 5–7 in Fig. 3) give z_{\max} larger than the cubic model value based on the experi-

ments reported here by ~4%. This is clearly beyond our experimental uncertainty since even the maximum possible temperature gradient of 2 $\mu^\circ\text{C}/\text{cm}$ can account for only 0.8%. We are unable to explain this 4% discrepancy.

Figure 4 is a deviation plot for contours 5–7 relative to the CM contour (line 8) after the latter together with the experimental data are scaled vertically by a factor 1.0415 so that the z_{\max} of contour 8 coincides with that of contour 7.

Table III shows that the disagreement in the susceptibility values corresponding to the contours 5–8 is as much as 5% without the scaling, i.e., when $a=22.3$ is used for the cubic model as in Fig. 3. Table III also shows the limits of variation of the parameter r along the χ contours. The values of k for SGS and HM are taken from the sources indicated; for the Kang-White (KW) contour, the value of k was taken from Ref. 29, where

TABLE III. Limiting values of the parameter r and susceptibility. Numbers in parentheses here correspond to those in Fig. 3. For the last line of the table, k is taken from Ref. 29.

	k	$r(T_{\min})$ (10^{-5})	$r(T_{\max})$ (10^{-5})	χ^{-1} 10^4 ($\text{erg cm}^3/\text{g}^2$)
(5) SGS (unrest. LM)	1.828	2.29	6.55	4.978
(6) SGS (rest. LM)	1.413	5.12	6.43	4.909
(7) HM (WE)				4.799
(8) KW (CM) with $a=22.3$	1.23	6.45	6.45	4.721

CO₂ thermodynamic data considerably removed from the critical point were analyzed on the basis of an unrestricted cubic model.

V. FURTHER DISCUSSION OF HEIGHT SCAN DATA

In Sec. IV, height profiles were considered only for the purpose of determining the (z, T) values at which the intensity was constant ($I = I_1$). In this section, we discuss further results of height scans, providing additional information on (1) the asymmetry of profiles of scattered intensity versus height between liquid and vapor phases below the critical temperature and (2) the relationship between the *peak* intensity (I_p) as a function of height and the temperature. This latter relationship enables an alternative estimation of the critical temperature.

Table IV shows the limiting intensities at the liquid-vapor interface below T_c for $T_c - T > 11$ m°C and the peak intensity above T_c , estimated from several height scans. For the subcritical temperatures, the intensity of

TABLE IV. Maximum intensities obtained from height profiles. I_L and I_V are scattered intensities from just below and just above the meniscus, respectively. I_p is the peak intensity obtained from a height scan near or above T_c . The number in parentheses is the probable error in the last digit(s): e.g., 29.5(10) = 29.5 ± 1.0.

Temperature (°C)	Day	I_L	I_V
30.8502(1)	71	1.721(14)	1.614(14)
30.8506(3)	72	1.757(14)	1.629(14)
30.9087(1)	32	2.85(2)	2.69(2)
30.9098(2)	29	2.93(3)	2.77(3)
30.9618(5)	50	5.7(1)	5.53(10)
30.9854(1)	79	12.9(3)	12.3(3)
30.9993(1)	26	29.5(10)	29.0(10)

		I_p
31.006 30(10)	10	70(5)
31.006 30(10)	16	68(4)
31.007 60(5)	37	83(4)
31.007 77(5)	48	82(5)
31.010 00(5)	4	155(10)
31.010 90(10)	11	255(10)
31.011 60(10)	19	343(5)
31.012 50(10)	20	325(4)
31.012 60(10)	40	341(7)
31.017 30(5)	1	145(2)
31.022 00(10)	36	102(1)
31.022 01(5)	61	107(1)
31.022 06(5)	15	99.5(10)
31.022 60(5)	17	94.5(10)
31.022 75(5)	18	94.5(10)
31.027 20(10)	13	72(1)
31.029 23(5)	8	65(1)
31.030 00(10)	22	62.7(3)
31.030 15(5)	67	65.7(5)
31.030 30(10)	38	62.8(4)
31.037 70(5)	45	46.9(3)
31.060 30(10)	24	25.1(1)

light scattered just below the meniscus (I_L) was always greater than that scattered just above the meniscus (I_V), and the difference increases with decreasing temperature. This phenomenon is due to the variation of the refractive index as a function of height, or equivalently as a function of the gravity-induced density gradient.¹⁰

Table V gives the detailed temperature behavior of the tops of some of the height profiles very close to the critical temperature as the temperature fluctuated a couple of tenths of a millidegree over any given day. The runs are typically separated by 1–2 h.

Some representative height scans for temperatures listed in Table IV that lay outside the range of the contour data are shown in Fig. 5. Figure 5, parts (1) and (2), shows large slopes (dI/dz) near the meniscus for temperatures just below the minimum value used for the contour. These slopes contributed appreciably to the uncertainties quoted for the corresponding values of I_L and I_V . Figure 5, parts (3)–(6), shows flattening of the height profiles farther below the contour range and above it.

The dependence of the limiting intensity I_p on temperature is shown in Fig. 6. The data points below 31.00°C represent $(I_L + I_V)/2$. The error bars below 31.00 and above 31.02 are not drawn because they are comparable in size to the diameter of the data circles. Intensities $I_p > 200$ are plotted on an expanded temperature scale in the insert where error bars are shown for these measurements of I_p . A portion of the error for $I_p > 200$ came from uncertainty of the PMT calibration for such large intensities, as discussed in Sec. III. Comparison of the runs of day 20 (open circles) and day 40 (solid circles) in the inset suggests an upward shift of the critical temperature by ~0.3 m°C, concurring with the overall drift of the contour toward higher temperature mentioned in Sec. IV. The maximum value of I_p as a function of temperature averaged over the two runs occurred at 31.0121 ± 0.0001

TABLE V. Finer detail very close to the critical temperature. Temperatures are indicated within each group in order of the runs, which were taken typically one or two hours apart.

Day	Run	Temperature (°C)	I_p
11	1	31.011 10(20)	282(3)
	2	31.010 90(5)	246(3)
	3	31.011 10(5)	271(3)
	4	31.010 84(5)	235(2)
19	1	31.011 75(5)	362(3)
	2	31.011 60(5)	356(3)
	3	31.011 60(10)	362(4)
	4	31.011 77(5)	377(4)
20	1	31.012 57(5)	313(3)
	2	31.012 47(5)	324(4)
40	1	31.012 40(10)	370(2)
	2	31.012 60(5)	366(4)
	3	31.012 55(5)	362(2)
	4	31.012 72(5)	343(2)
	5	31.012 65(5)	343(3)

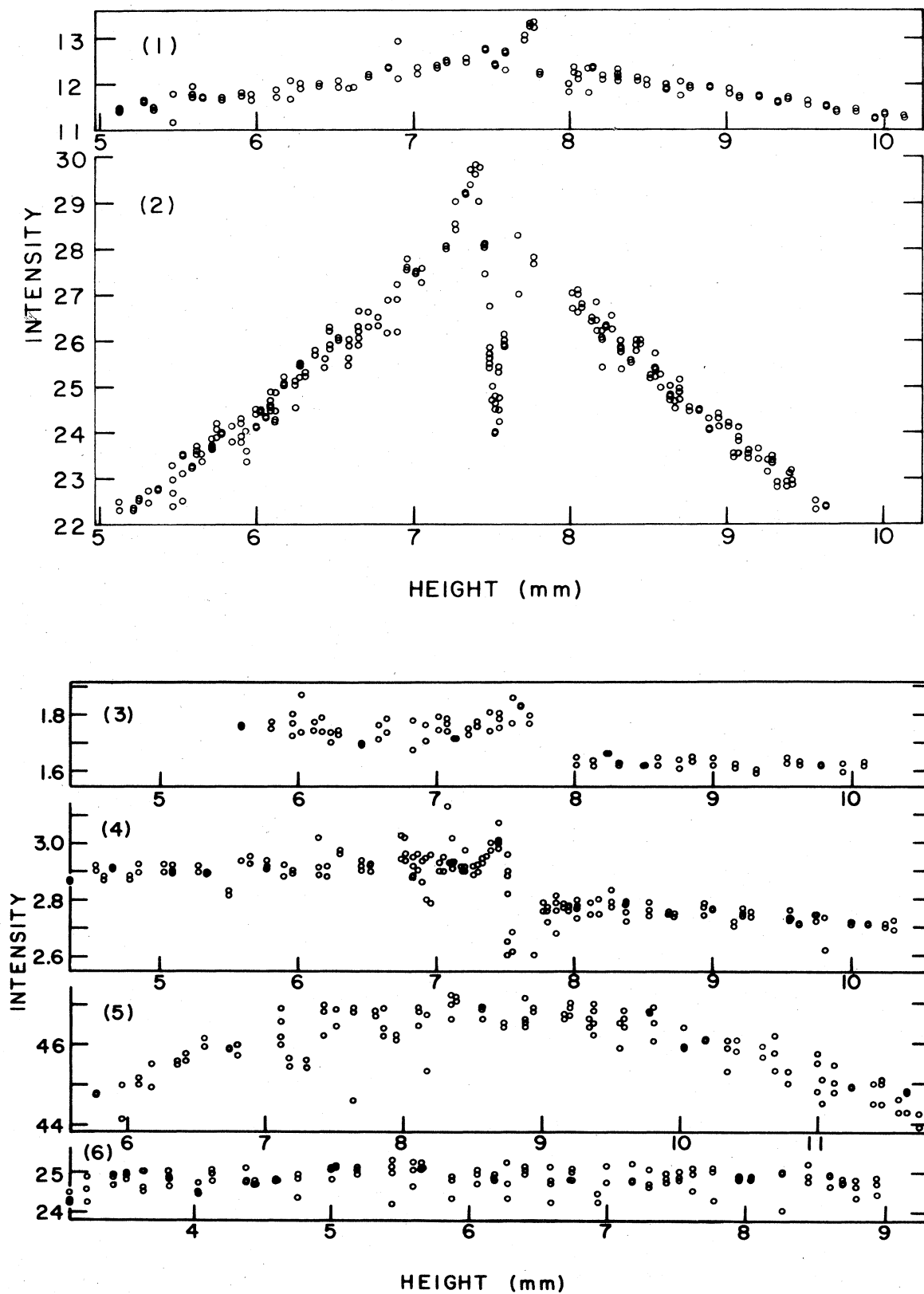


FIG. 5. Height profiles outside the contour temperature range. (1) and (2), just below T_{\min} ; (3)–(6), regions considerably removed from T_c . The temperatures in $^{\circ}\text{C}$ are (1) 30.9854 ($\Delta T = -0.0261$), (2) 30.9993 ($\Delta T = -0.0122$), (3) 30.8506 ($\Delta T = -0.1610$), (4) 30.9098 ($\Delta T = -0.1017$), (5) 31.0377 ($\Delta T = 0.0261$), (6) 31.0603 ($\Delta T = 0.0488$).

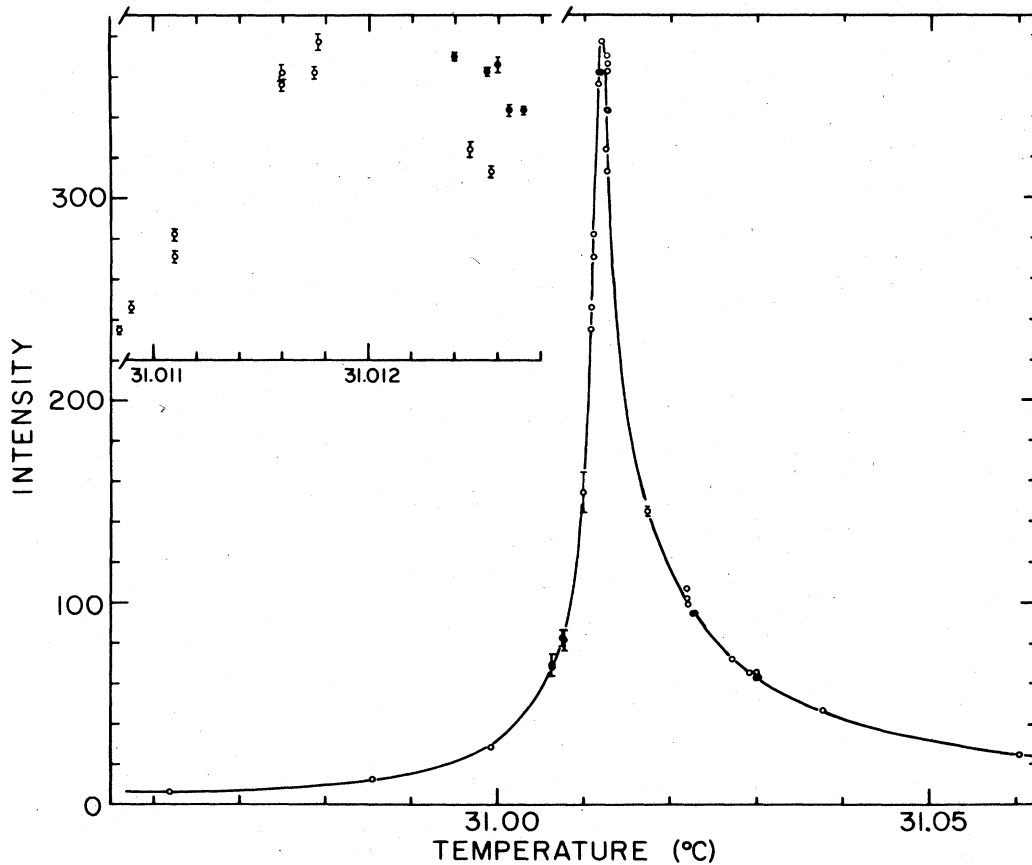


FIG. 6. Peak intensity as a function of temperature. The probable errors in the intensity measurements for $I > 200$ are shown in the inset. Solid and open circles in the inset differentiate data taken approximately 3 weeks apart.

which is ~ 0.6 m°C higher than T_c obtained by fitting the CM parametric equation. This result is to be expected based on the work of Dobbs and Schmidt,³⁰ and Splittorff and Miller,³¹ according to which, for finite cross sections of the laser beam (diameter ~ 0.1 mm) centered on the meniscus or the layer of the fluid at the critical density,

the scattering at a given angle is maximum at a temperature somewhat higher than T_c .

ACKNOWLEDGMENTS

This research was supported in part by the Office of Naval Research.

*Present address: 8109 Broadview Drive, Frederick, MD 21701.

†To whom reprint requests should be addressed.

- ¹J. A. White, R. W. Freeman, and B. S. Maccabee, *Bull. Am. Phys. Soc.* **18**, 725 (1973).
- ²J. A. White and B. S. Maccabee, *Phys. Rev. A* **11**, 1706 (1975).
- ³B. D. Josephson, *J. Phys. C* **2**, 1113 (1969).
- ⁴P. Schofield, *Phys. Rev. Lett.* **22**, 606 (1969).
- ⁵P. Schofield, J. D. Litster, and J. T. Ho, *Phys. Rev. Lett.* **23**, 1098 (1969).
- ⁶J. T. Ho and J. D. Litster, *Phys. Rev. B* **2**, 4523 (1970).
- ⁷R. Hocken and M. R. Moldover, *Phys. Rev. Lett.* **37**, 29 (1976).
- ⁸P. Kang and J. A. White, *Bull. Am. Phys. Soc.* **21**, 685 (1976).
- ⁹P. Kang and J. A. White, *Bull. Am. Phys. Soc.* **22**, 619 (1977).
- ¹⁰P. Kang, Ph.D. dissertation, American University, 1976.
- ¹¹L. S. Ornstein and F. Zernike, *Proc. K. Ned. Akad. Wet.* **17**, 793 (1914).
- ¹²H. M. J. Boots, D. Bedeauz, and P. Mazur, *Physica (Utrecht)* **84A**, 217 (1976).

- ¹³B. S. Maccabee and J. A. White, *Phys. Lett.* **35A**, 187 (1971); *Phys. Rev. Lett.* **27**, 495 (1971).
- ¹⁴J. H. Lunacek and D. S. Cannell, *Phys. Rev. Lett.* **27**, 841 (1971).
- ¹⁵H. B. Tarko and M. B. Fisher, *Phys. Rev. B* **11**, 1217 (1975).
- ¹⁶E. Brezin, J. C. Le Guillou, and J. Zinn-Justin, in *Phase Transitions and Critical Phenomena*, edited by C. Domb and M. S. Green (Academic, New York, 1976), Vol. 6.
- ¹⁷M. R. Moldover, J. V. Sengers, R. W. Gammon, and R. J. Hocken, *Rev. Mod. Phys.* **51**, 79 (1979).
- ¹⁸From the Lorentz-Lorenz formula. See, e.g., M. Born and E. Wolf, *Principles of Optics* (Pergamon, Oxford, 1980).
- ¹⁹J. A. White and B. S. Maccabee, *Phys. Rev. Lett.* **26**, 1468 (1971).
- ²⁰M. Giglio and A. Vendramini, *Phys. Rev. Lett.* **34**, 561 (1975).
- ²¹D. L. Madison and J. A. White, *Bull. Am. Phys. Soc.* **23**, 312 (1978).
- ²²P. C. Hohenberg and M. Barmatz, *Phys. Rev. A* **6**, 289 (1972).

- ²³T. A. Murphy, J. V. Sengers, and J. M. H. Levelt Sengers, in *Proceedings of the Sixth Symposium on Thermophysical Properties*, edited by P. E. Liley (ASME, New York, 1973).
- ²⁴J. M. H. Levelt Sengers, W. L. Greer, and J. V. Sengers, *J. Phys. Chem. Ref. Data* **5** (1976).
- ²⁵L. Wilcox and W. T. Estler, *J. Phys. (Paris) Colloq.* **32**, C5A-175 (1971).
- ²⁶R. Hocken (private communication).
- ²⁷W. T. Estler, R. Hocken, T. Charlton, and L. R. Wilcox, *Phys. Rev. A* **12**, 2118 (1975).
- ²⁸A set of parameters for use with the CM equation is $a=21.7$, $\gamma=1.240$, $\beta=0.325$, $b^2=3/(3-2\beta)=1.277$ (see Ref. 17, Table II).
- ²⁹B. S. Maccabee and J. A. White, *Phys. Lett.* **49A**, 69 (1974).
- ³⁰B. C. Dobbs and P. W. Schmidt, *Phys. Rev. A* **7**, 741 (1973).
- ³¹O. Splittorff and B. N. Miller, *Phys. Rev. A* **9**, 550 (1974).